Life-Cycle Analysis and Assessment in Civil Engineering: Towards an Integrated Vision – Caspeele, Taerwe & Frangopol (Eds)
ISBN 978-1-138-62633-1

A simple estimation method of the probability distribution of residual displacement and maximum bending moment for pile supported wharf by earthquake

T. Nagao
Research Center for Urban Safety and Security, Kobe University, Kobe, Japan

P. Lu
Graduate School of Engineering, Kobe University, Kobe, Japan

ABSTRACT It is necessary to conduct two-dimensional nonlinear earthquake response analysis many times in order to evaluate probabilistic characteristic of residual deformations and maximum bending moment of a pile supported wharf by earthquake. This paper aims at proposing a simple estimation method for those parameters of pile supported wharf. Variations of input earthquake ground motion were evaluated based on the variations of site amplification factors. It was shown that the probability distributions of residual deformations and maximum bending moment of a pile supported wharf can be evaluated with enough accuracy by using the result of three earthquake response analyses.

1 INTRODUCTION

Technical standards for civil engineering works in Japan introduced two-stage design input earthquake ground motions after the 1995 Kobe earthquake. One of the two-stage design earthquake ground motions is called as the Level-one earthquake ground motions which presumably occur with certain degree of frequency during the design working period of infrastructure. The earthquake ground motions correspond to the reference earthquake ground motions for evaluating serviceability of structures specified in ISO23469. Technical standards for port and harbor facilities applies reliability-based design for earthquake resistant design of wharves against the Level-one earthquake ground motions.

Earthquake ground motions can be expressed by the multiplication of source, path and site amplification characteristics in the frequency domain (e.g. Nagao et al. 2012). Among the three characteristics, site amplification characteristic is known to greatly differ from site to site (e.g. Nozu et al. 2008). Therefore, probability distribution of earthquake ground motion is thought to greatly differ from site to site. However, the technical standards for port facilities does not take the variation of input seismic motion at the site of interest into account for the reliability-based design of wharves.

It is necessary to evaluate both the residual displacement and the maximum bending moment generated in piles for the earthquake resistant design of pile supported wharves. As pile supported wharves are constructed on coastal soft ground, residual deformation occurs in soil layers by earthquake. It should be noted that both the residual displacement and the maximum bending moment of pile supported wharves are strongly affected by the deformation of the ground (Nagao and Oda 2017). Therefore, two-dimensional finite element earthquake response analysis considering both the non-linear characteristics and the effects of liquefactions of soil layers must be used for the evaluation of the residual displacement and the maximum bending moment for pile supported wharves. The problem of the application of that kind of analysis is the computational load. The computational load is particularly noteworthy in cases where probability distribution of those indices shall be evaluated because designers must conduct that time-consuming analyses many times in order to calculate the probability distribution.

Nagao (2009) conducted a study on a simple evaluation method of seismic reliability index considering the variation of the soil strength. Hirai and Nagao (2016) conducted a study on a simple estimation method of probability distribution of residual displacement of gravity-type quay wall considering the variation in earthquake ground motion.

This study aims at proposing a simple estimation method of probability distribution of residual displacement and the maximum bending moment of pile supported wharves considering the variation in earthquake ground motion. We conducted two-dimensional finite element earthquake response analyses by using 136 input seismic motions considering the variations in the site amplification factors and obtained the probability distribution of residual displacement and the maximum bending moment of pile supported wharves. The probability distribution of residual displacement and the maximum bending moment was approximated by the lognormal distribution. Next, we calculated the average and the standard deviation of the Fourier amplitude spectrum of input seismic motions and evaluated three input seismic motions corresponding to the average, average plus and minus standard deviation. We finally proposed a simple estimation method of the probability distribution of the indices by using the result of three input seismic motions.

2 STUDY METHOD

In this study, the variation of earthquake ground motions is considered as the variation of site amplification factors at the port of Sendai-Shiogama in Japan. Earthquake ground motion data observed at two strong motion observation sites of K-NET (Kinoshita 1998) are used for the study. The location of the strong motion observation sites are shown in Figure 1.

As earthquake ground motions can be expressed by the multiplication of source, path and site amplification characteristics in the frequency domain (e.g. Nagao et al. 2012), taking the strong motion observation site MYG012 as a target site and MYG013 as a reference site, the site amplification factor at MYG012 is evaluated by the following equation with the strong motion records at MYG012 and MYG013 by the same event.

$$G_{MYG012}(f) = G_{MYG013}(f)\frac{O_{i,MYG012}R_{i,MYG012}}{O_{i,MYG013}R_{i,MYG013}} \tag{1}$$

where, f is frequency, G_j is the amplification factor at site j, O_{ij} is Fourier amplitude spectrum of seismic motion record of earthquake i at site j, R_{ij} is hypocentral distance of earthquake i and site j. O_{ij} is calculated as a square root of mean of sum of squared NS component and squared EW component.

Here, site amplification factor at the reference site was obtained by Nozu and Nagao (2003).

In order to avoid the effect of nonlinearity of the ground and to eliminate the data with poor S/N ratio, earthquake ground motion record with JMA magnitude in the range between 4.0 and 7.0 and with sufficient S/N ratio from 0.2Hz to 10Hz in Fourier ampli- tude spectrum were chosen for the study. 68 events were picked up for the study.

Figure 2 shows the variation of calculated Fourier amplitude spectrum of the earthquake ground motion with site amplification factor calculated by equation (1). The logarithmic mean (hereafter written as λ) of the 68 Fourier amplitude spectrum is shown with a red solid line and the logarithmic mean plus and minus logarithmic standard deviation are shown with blue lines in the figure. The logarithmic standard deviations (hereafter written as ξ) are different from frequency to frequency.

The variation of group delay time is considered as phase characteristics. The group delay time is defined as a derivative of Fourier phase spectrum with

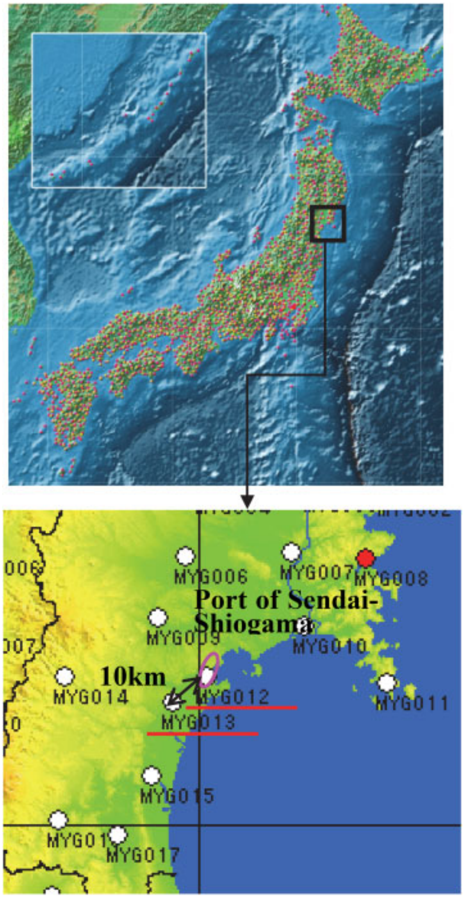

Figure 1. Location of the strong motion observation sites.

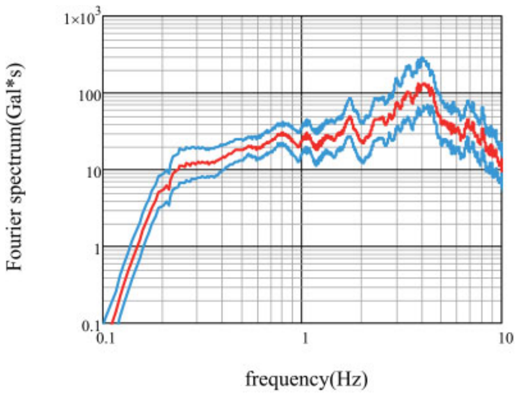

Figure 2. Variation of the Fourier spectrum.

respect to angular frequency as the following equation (Sawada et al. 2000).

$$T_{gr}(\omega) = \frac{d\phi(\omega)}{d\omega} \tag{2}$$

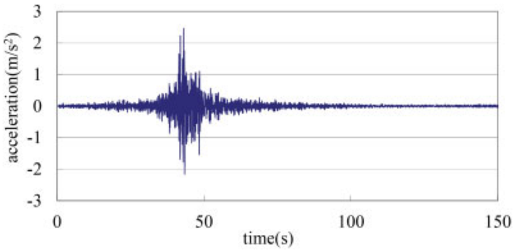

Figure 3. Example of earthquake ground motion.

where ϕ is Fourier phase spectrum, ω is angular frequency. The group delay times are prepared for earthquake response analysis by the following equation.

$$T_{grn}(\omega) = (1+r)T_{gr0}(\omega) \tag{3}$$

where T_{grn} is the group delay time of nth analysis, r is random variable with normal distribution whose mean is zero and standard deviation is 0.3. The group delay time of the Level-one earthquake ground motion at the port of Sendai-Shiogama is used as T_{gr0}. Two group delay times are generated for each single site amplification factor. By coupling the group delay times and the site amplification factors, 136 input motions are generated. Figure 3 shows the earthquake ground motion calculated with the mean of site amplification factor and the mean of group delay time.

The wharf being addressed here has a rigid-frame structure as shown in Figure 4, and the one with the steel pipe pile foundation has a structure with its mass concentrated upon the superstructure.

Earthquake response of the wharf was evaluated by use of the two-dimensional earthquake response effective stress analysis. The code applied in this study is FLIP (Iai et al. 1990), which is frequently used for the evaluation of the seismic response of the ground and quay walls (e.g. Tamari et al. 2015) because it well reproduces the seismic response of quay walls damaged by earthquake such as those damaged by the 1995 Kobe earthquake. Parameters for analysis models are set according to the standard method established for the code (Morita et al. 1997). Piles and superstructures are modeled as nonlinear beam elements.

Soil parameters are shown in Table 1. Replacement sand is liquefiable.

Table 1. Soil parameters.

	Thickness (m)	Density (t/m^3)	Internal friction angle(degree)
Soil 1	3.0	1.45	30
Soil 2	7.0	1.45	30
Soil 3	4.0	1.45	30
Soil 4	9.0	1.45	30
Soil 5	11.0	2.00	44
Replacement sand	9.0	1.84	41

3 STUDY RESULTS

Figure 5 shows the relationship between peak ground acceleration (PGA) of the input seismic motion and displacement of the wharf. Although the inertial force is in proportion to the acceleration, there exists a large variation between the peak ground acceleration and the residual displacement. This is because the displacement of the wharf is strongly affected by the deformation of soil layers. Figure 6 shows the relationship between peak ground velocity (PGV) of the input seismic motion and displacement of the wharf. There exists a variation between the two parameters although the degree of variation is low compared with that between peak ground acceleration and residual displacement.

Adequate index for evaluating the residual displacement was found to be the sum of Fourier amplitude spectrum in the range between 0.5 to 5.0 Hz. Figure 7 shows the relationship between the sum of Fourier amplitude spectrum in the range between 0.5 to 5.0 Hz and residual displacement. It is obvious that the degree of variation is lowest among the three parameters. Here, the frequency range was decided considering the governing frequency range of the seismic motion to the deformation and section forces of structures.

Blue diamonds in Figure 7 is the result by the seismic motion of the Fourier amplitude of logarithmic mean (λ) plus and minus x times logarithmic standard deviation (ζ) where $x = 0$, 0.5, 0.75 and 1.0.

Figure 8 shows the relationship between the sum of Fourier amplitude spectrum in the range between 0.5 to 5.0 Hz and maximum bending moment generated in piles. It is obvious that not only the residual displacement but the maximum bending moment can be evaluated by using the sum of Fourier amplitude spectrum. Note that the full plastic bending moment of the foundation pile is 482.5 kNm/m and therefore all the piles are in elastic situation during earthquake.

Although the displacement and the maximum bending moment by the seismic motion with x times logarithmic standard deviation match those by each seismic motion, it should be noted that the displacement and the maximum bending moment by the seismic motion with mean Fourier amplitude does not coincide with the average values of each seismic motion. Same can be pointed out to the results by the seismic motion with mean plus and minus x times logarithmic standard deviation. For example, seismic motion with average Fourier amplitude spectrum has average amplitude at each frequency. On the contrary, each seismic motion has larger amplitude or smaller amplitude compared with the average amplitude at each frequency. Residual displacement and maximum bending moment are thought to be strongly affected by the large amplitude component of seismic motion. Small amplitude component of seismic motion is thought to have little effect on residual displacement and maximum bending moment. The reason of the disagreement can explained for this reason.

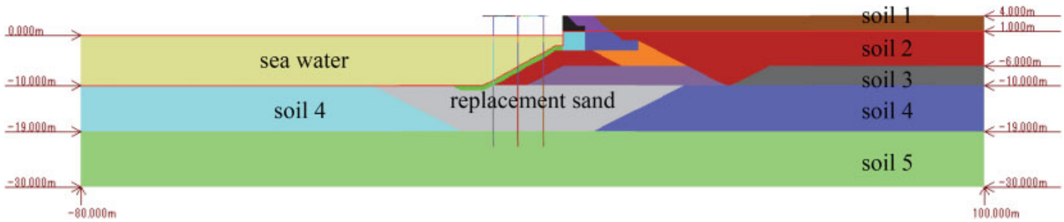

Figure 4. Profile of the study target wharf.

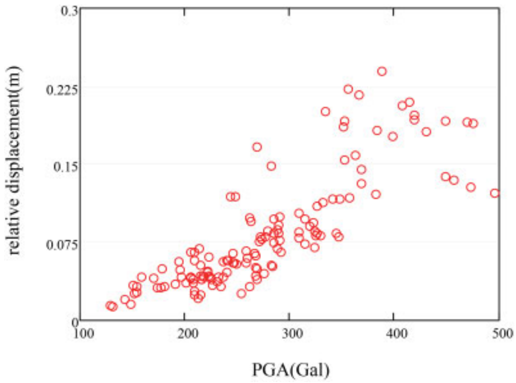

Figure 5. Relationship between PGA and residual displacement.

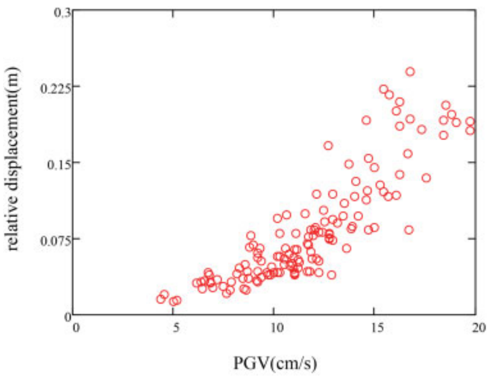

Figure 6. Relationship between PGV and residual displacement.

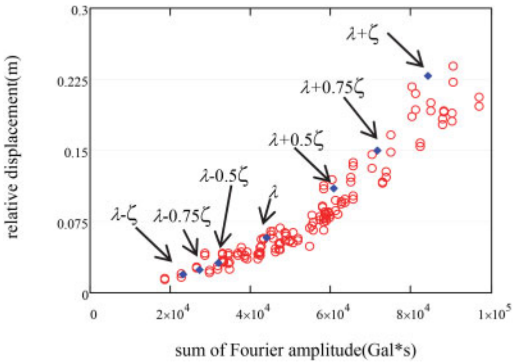

Figure 7. Relationship between sum of Fourier amplitude and residual displacement.

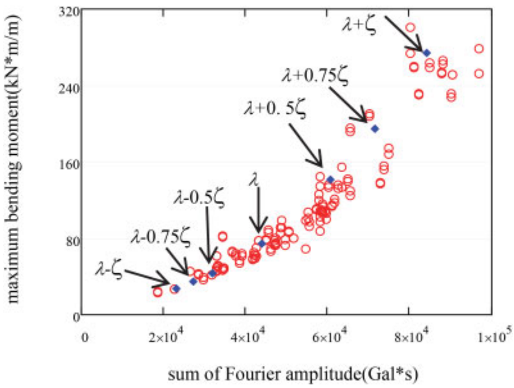

Figure 8. Relationship between sum of Fourier amplitude and maximum bending moment.

Therefore, the following equation is proposed as the index of the magnitude of the sum of Fourier amplitude spectrum.

$$x' = \frac{amp - \lambda_{amp136}}{\zeta_{amp136}} \tag{4}$$

where *amp* is the sum of the Fourier amplitude spectrum with the range from 0.5Hz to 5.0Hz, λ_{amp136} and ζ_{amp136} are the logarithmic mean and the logarithmic standard deviation of the sum of the Fourier amplitude spectrum of the 136 earthquake ground motions respectively.

The relationship between the sum of the Fourier amplitude spectrum and the residual displacement are shown in Figure 9. Also, Figure 10 shows the relationship between the sum of the Fourier amplitude spectrum and the maximum bending moment of the piles. It was found that average and average plus or minus seismic motion correspond to average minus 0.5ζ and average plus or minus 1.7ζ of each seismic motion respectively.

Assuming the linear relationship between x' and displacement or maximum bending moment, by using the least squared approximation, average and average plus or minus standard deviation of displacement and maximum bending moment were estimated by the

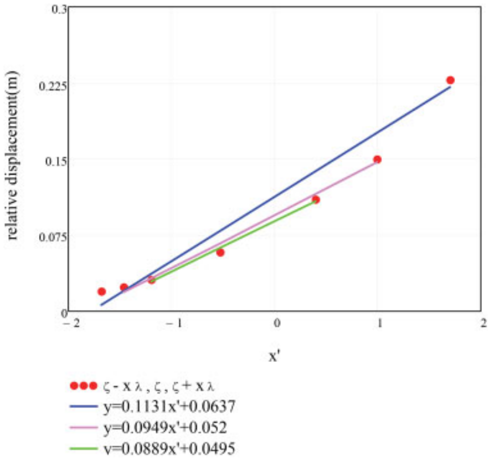

Figure 9. Estimation of mean and standard deviation of displacement.

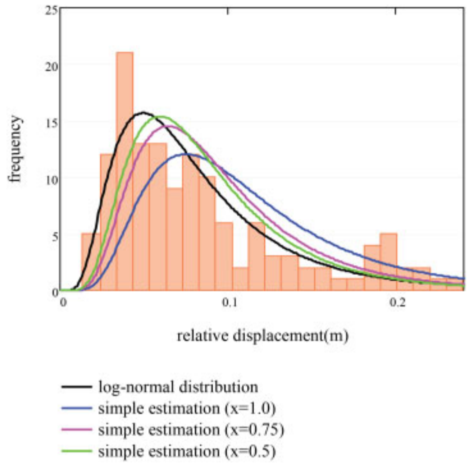

Figure 11. Estimation of probability distribution of displacement.

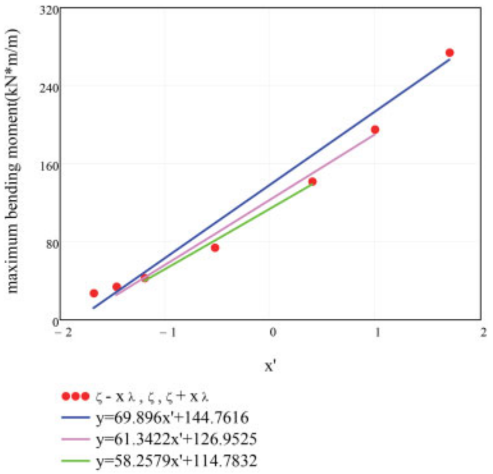

Figure 10. Estimation of mean and standard deviation of maximum bending moment.

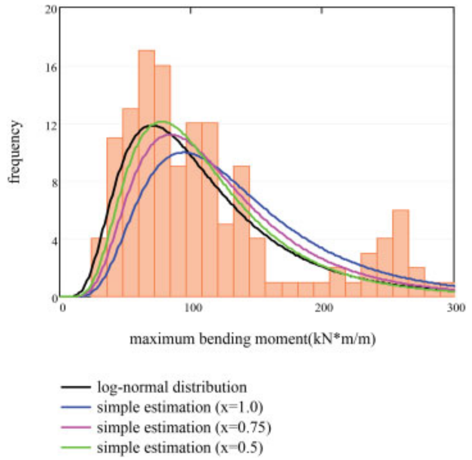

Figure 12. Estimation of probability distribution of maximum bending moment.

regression equations shown in the figures. Here, the blue solid line, the purple solid line and the green solid line are the cases where $x = 1.0$, 0.75 and 0.5 respectively.

Figure 11 and 12 show the estimated probability distribution of displacement and maximum bending moment respectively. Histograms in the figures show the results by each seismic motion. Black solid lines show the probability distribution of the results by each seismic motion assuming the lognormal distribution. The blue solid lines, the purple solid lines and the green solid lines are the estimated probability distributions assuming the lognormal distributions, where $x = 1.0$, 0.75 and 0.5 respectively.

It can be pointed out that both residual displacement and maximum bending moment can be estimated with enough accuracy by using the three results of earthquake response analysis.

Figure 13 and 14 show the estimated cumulative probability distribution of displacement and maximum bending moment respectively. Orange dotted lines show the cumulative probability distribution by each seismic motion. Black dashed lines show the cumulative probability distribution of the results by each seismic motion assuming the lognormal distribution. The blue solid lines, the purple solid lines and the green solid lines are the estimated cumulative probability distributions assuming the lognormal distributions, where $x = 1.0$, 0.75 and 0.5 respectively.

In the reliability analysis, reproduction of the right side tail of the probability distribution is important because the allowable failure probability of displacement and maximum bending moment for structures are set to as reasonably low as possible. From Figure 13 and 14, it can be pointed out that the simple estimation method by use of average and average plus and

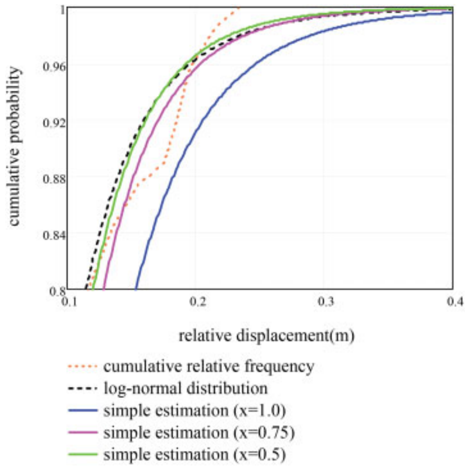

Figure 13. Estimation of cumulative probability distribution of displacement.

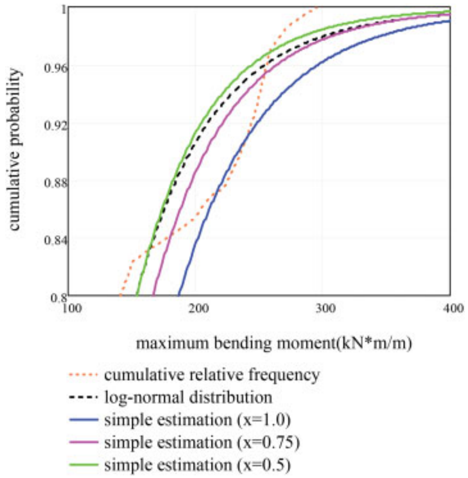

Figure 14. Estimation of cumulative probability distribution of maximum bending moment.

minus 0.75 times standard deviations enables to estimate probability distributions of residual displacement and maximum bending moment on the conservative side with enough accuracy and the method is highly applicable to the practical design.

4 CONCLUSIONS

In this paper, a simple estimation method for probability distribution of residual displacement and maximum bending moment generated in piles of open-type wharf by earthquake was discussed using finite element earth-quake response analysis. As residual displacement and maximum bending moments of the wharf is strongly influenced by the deformation of soil layers, sum of Fourier amplitude spectrum in the range between 0.5 to 5.0 Hz was used for the indicator to evaluate displacement and maximum bending moment.

A simple estimation method for probability distribution of residual displacement and maximum bending moment was proposed by using the results of three earthquake response analysis: seismic motions whose amplitude correspond to average, average plus and minus 0.75 times standard deviations. It was shown that the proposed method enables to estimate probability distributions of residual displacement and maximum bending moment on the conservative side with enough accuracy and the method is highly applicable to the practical design.

ACKNOWLEDGEMENTS

The authors would like to thank Dr. Hirai for his useful advice in conducting this study. The authors would also like to thank National Research Institute for Earth Science and Disaster Resilience (NIED) for providing seismic data observed by K-NET.

REFERENCES

Hirai, T. and Nagao, T. 2016. A Simple Estimation Method of the Probability Distribution of Residual Deformation of Gravity Type Quay Walls Considering the Variation of Earthquake Ground Motion, *Proc. of IALCCE2016*, pp. 485–491.

Iai, S. and Matsunaga, Y. and kameoka, T. 1990. Space Plasticity Model for Cyclic Mobility. *Report of Port and Harbor Research Institute*, 27(4): 27–56.

Kinoshita, S. 1998. Kyoshin Net (K-net), *Seim. Res. Lett.*, **69**, 309–332.

Morita, T.,Iai, S., Liu, H.,Ichii, K. and Sato, Y. 1997. Simplified method to determine parameter of FLIP. *Technical Note of The Port and Harbor Research Institute*, No. 869 (in Japanese).

Nagao, T. 2009. A Study on a Simple Estimation Method of Seismic Reliability Indices against Residual Deformation for Quay Walls. *Proc. of ICOSSAR'09*.

Nagao, T. and Yamada, M. and Nozu, A. 2012. Probabil- istic Seismic Hazard Analysis with Focus on Fourier Amplitude and Group Delay Time. *Proc. of the 15th World Conf. on Earthquake Engineering*, No. 468.

Nagao, T. and Oda, T. 2017. Evaluation of the Damage Level of Open-Type Wharf by Earthquake Focusing on the Natural Frequency, *Proc. of ICOSSAR2017*.

Nozu, A., Nagao, T. and Yamada, M. 2008. A strong motion simulation method suitable for areas with less information on subsurface structure, *Proc. of the 14th World Conf. on Earthquake Engineering*.

Nozu, A. and Nagao, T. 2003. Site Amplification Factors for Strong-Motion Sites in Japan Based on Spectral Inversion Technique. *Technical Note of The Port And Airport Research Institute*, No. 1112. (in Japanese).

Sawada, S. and Morikawa, H. and Toki, K. and Yoko yama, K. 2000. Identification of Path and Local Site Effects on Phase Spectrum of Seismic Ground Motion. *Proc. of the 12th World Conf. on Earthquake Engineering*, No. 683.

Y. Tamari, J. Hyodo, K. Ichii, T. Nakama and A. Hosono. 2015. Seismic ground behavior in Tokyo part at the 2011 off pacific coast of Tohoku earthquake, *6th International conference on earthquake geotechnical engineering.*